NEOPLASIA
www.neoplasia.com

Volume 10 Number 12 December 2008 pp. 1373–1382 1373

Tumor Progression and Oncogene Addiction in a PDGF-B–Induced Model of Gliomagenesis[1,2]

Filippo Calzolari[*,†,3], Irene Appolloni[*,†,3], Evelina Tutucci[*,†], Sara Caviglia[*,†], Marta Terrile[*,†], Giorgio Corte[*,†] and Paolo Malatesta[*,†]

*National Institute for Cancer Research (IST), IRCCS, Largo Rosanna Benzi 10, 16132 Genoa, Italy; [†]Department of Oncology and Genetics (DOBIG), University of Genoa, Largo Rosanna Benzi 10, 16132 Genoa, Italy

Abstract

Platelet-derived growth factor B (PDGF-B) overexpression induces gliomas of different grades from murine embryonic neural progenitors. For the first time, we formally demonstrated that PDGF-B–induced neoplasms undergo progression from nontumorigenic low-grade tumors toward highly malignant forms. This result, showing that PDGF-B signaling alone is insufficient to confer malignancy to cells, entails the requirement for further molecular lesions in this process. Our results indicate that one of these lesions is represented by the down-regulation of the oncosuppressor *Btg2*. By *in vivo* transplantation assays, we further demonstrate that fully progressed tumors are PDGF-B–addicted because their tumor-propagating ability is lost when the *PDGF-B* transgene is silenced, whereas it is promptly reacquired after its reactivation. We provide evidence that this oncogene addiction is not caused by the need for PDGF-B as a mitogen but, rather, to the fact that PDGF-B is required to overcome cell-cell contact inhibition and to confer *in vivo* infiltrating potential on tumor cells.

Neoplasia (2008) 10, 1373–1382

Introduction

Gliomas are a heterogeneous group of almost incurable cancers. They are classified according to their histopathologic features and to the expression of markers of different glial lineages, into astrocytomas, oligodendrogliomas, mixed oligoastrocytomas and glioblastomas. The latter is the most malignant form and is commonly regarded as the highest grade of astrocytoma [1,2], although it has been recently proposed that some glioblastomas may instead represent high-grade oligodendrogliomas [3]. The diversity of gliomas is mirrored by the number of different signaling pathways shown to play roles in the generation of these tumors [1,4,5].

A common molecular lesion found in gliomas of different histopathological grades is the alteration of platelet-derived growth factor B (PDGF-B) signaling [6–8]. The relevance of this signaling pathway to the process of gliomagenesis has been demonstrated by studies in the mouse, where both perinatal and adult progenitor/stem cells can be induced to generate oligodendrogliomas, astrocytomas, and glioblastomas by forced overexpression of PDGF-B [9–15]. Despite this wealth of data, it is still unclear whether and how PDGF-B signaling contributes to processes beyond tumor initiation, such as the acquisition and the maintenance of progressively more malignant phenotypes.

In our work, we investigated these issues and demonstrated that PDGF-B–induced tumors acquire malignant features, progressing from low- to high-grade lesions, and that the down-regulation of the oncosuppressor *Btg2* is involved in this process. Furthermore, by loss- and gain-of-function approaches, we show that continued PDGF-B overexpression is necessary for the maintenance of the tumorigenic activity of the fully progressed tumor cells, which therefore results addicted to PDGF-B and never acquire independency from the initiating stimulus.

Abbreviations: IRES, internal ribosome entry site; GFP, green fluorescent protein; GFAP, glial fibrillary acidic protein

Address all correspondence to: Paolo Malatesta, National Institute for Cancer Research (IST), IRCCS, Largo Rosanna Benzi 10, 16132 Genoa, Italy.
E-mail: paolo.malatesta@istge.it

[1]This work was supported by AIRC (Associazione Italiana per la Ricerca sul Cancro) New Unit StartUp grant (*In vivo* screening for genes implicated in glioma formation and development of new animal models of glial tumors.) and by Fondazione Cassa di Risparmio di Genova grant (Basi molecolari e cellulari dei gliomi: individuazione di marcatori diagnostici e di nuovi bersagli terapeutici).

[2]This article refers to supplementary materials, which are designated by Table W1 and Figure W1 and are available online at www.neoplasia.com.

[3]Calzolari F. and Appolloni I. contributed equally to this work.

Received 17 July 2008; Revised 11 September 2008; Accepted 12 September 2008

DOI 10.1593/neo.08814

Materials and Methods

Cell Cultures

Cultures from tumors were established microdissecting green fluorescent protein (GFP)–positive areas under the fluorescence microscope and trypsinizing them for 20 minutes. All tumor cultures were maintained in DME-F12 added with B27 supplement and human recombinant fibroblast growth factor 2 and epidermal growth factor (20 ng/ml; Invitrogen, Carlsbad, CA) and plated on to Matrigel-coated flasks (1:200; BD Biosciences, San Jose, CA). For immunohistochemistry, cells were plated onto 13-mm-diameter coverslips coated with poly-D-lysine and fixed in 4% paraformaldehyde 2 days after.

For growth curve analyses and focus formation assays, 10^5 cells were plated within 35-mm-diameter Matrigel-coated wells and then either counted after trypsinization at the indicated time points or allowed to overgrow and be monitored for the presence of cell foci. Each condition/time point was analyzed in triplicate cultures.

Fluorescent Activated Cell Sorting

Acutely dissociated and cultured tumor cells were sorted using a FACSAria (BD Biosciences, Inc.). Purified GFP-positive and GFP-negative cell populations were visually inspected after sorting under a fluorescent microscope to quantify the contaminating fraction, which was <1% in most cases analyzed.

Retroviral Vectors and Transduction Procedures

The cDNA of mouse PDGF-B, derived from the RCAS-pBIG plasmid (kindly provided by Dr. E. Holland, Memorial Sloan-Kettering Cancer Center, New York), was inserted into the *Sal*I site of the pCEG retroviral vector (kindly provided by Gordon Fishell, The Skirball Institute of Biomolecular Medicine, New York) and into the blunted *Pme*I/*Sfi*I sites of the pCAG:Ds-Red vector (kindly provided by Dr. M. Goetz, Institute of Stem Cell Research, Germany), upstream the internal ribosome entry site (IRES)–Ds-Red reporter cassette. All the PDGF-B overexpression experiments, *in vitro* and *in vivo*, were carried out using the IRES-containing retroviral vector, in which the coding sequences for GFP or Ds-Red were downstream the IRES. Control experiments were performed using the retroviral vectors coding the reporters alone or the β-glucuronidase gene (*GUS*).

Replication-defective retroviral supernatants were prepared by transiently transfecting plasmids into Phoenix packaging cells as described elsewhere [16]. Retroviral vectors where used on cultured cells as previously described in the study of Heins et al. [17] and *in vivo* as described in the study of Appolloni et al. [18].

Animal Procedures

Mice were handled in agreement with the guidelines conforming to the Italian current regulations regarding the protection of animals used for scientific purposes (D.lvo 27/01/1992, n. 116). Procedures were specifically approved by the Ethical Committee for Animal Experimentation of the National Institute of Cancer Research and by the Italian Ministry of Health. All experiments have been performed on the C57/Bl6 mouse strain.

In utero intraventricular injections were performed as described elsewhere [19]. Animals injected at embryonic stages were let develop to term, and after birth, they were monitored for the appearance of symptoms indicating the presence of brain tumors. At first signs of symptoms, the animals were killed and perfused with 4% paraformaldehyde. The brains were photographed on a transilluminator and/or cryoprotected in 20% sucrose and sectioned with a Leica CM1100 cryostat (Wetzlar, Germany).

Tumor cells were injected in deeply anesthetized adult animals mounted on a stereotaxic apparatus. Up to 5 μl of cell suspension for each mouse, containing 50 to 50,000 cells, were injected using a Hamilton syringe (Bregma coordinates: AP, 1.0 mm; L, 1.5 mm left and 2.5 mm below the skull surface). Reabsorbable suture was used before awakening the animals. Animals were then monitored daily for the onset of neurologic symptoms.

Immunostaining

Immumostainings on brain sections or cultured cells were performed using the following antibodies: mouse monoclonal antibodies against Nestin (1:250; BD Pharmingen, San Diego, CA); glial fibrillary acidic protein (GFAP, 1:200; Sigma, St. Louis, MO), adenomatous polyposis coli (APC, 1:100, CC1; Calbiochem, San Diego, CA), BrdU (1:50; Bio-science Products AG, Emmenbruecke, Switzerland); rabbit polyclonal antibodies against Olig2 (1:200; Sigma), Ng2 (1:300; Chemicon-Millipore, Billerica, MA), and Sox2 (1:500; Chemicon-Millipore); chicken polyclonal antisera against GFP (1:500; Abcam, Cambridge, United Kingdom); and rat monoclonal antibodies against PDGFRα (1:100; BD Pharmingen) and Ki67 (1:25, tec3 clone; Dako, Glostrup, Denmark). Binding of primary antibodies was revealed with appropriate secondary fluorescein isothiocyanate– and tetramethyl rhodamine isothiocyanate–conjugated antibodies (1:50; Immucor, Norcross, GA) or biotinylated secondary antibodies (1:50; Dako), which were revealed with streptavidin-conjugated Alexa 488 (1:500; Molecular Probes-Invitrogen). Nuclei were stained through 5 minutes of incubation in DAPI solution (1 μg/ml; Sigma).

Immunostainings were examined with an Eclipse 800i (Nikon, Tokyo, Japan). Images were acquired with Nikon Digitalsight DS-M5c camera and analyzed with ImageJ (W.S. Rasband, ImageJ, US National Institutes of Health, Bethesda, MD; http://rsb.info.nih.gov/ij/, 1997-2007).

Data Analysis on Brain Sections and Cultured Cells

The means and SEs were calculated from different experiments. "*n*" denotes the number of animal used for *in vivo* experiments. The threshold for statistical significance, which was determined with a 2-tailed Student's *t* test, was considered as $P < .05$.

Real-time Polymerase Chain Reaction

Genomic DNA from sorted GFP-positive and GFP-negative cells was obtained by lysing the cells in 100 mM Tris-Cl pH 8.5, 5 mM EDTA, 0.2% SDS, 200 mM NaCl, and 100 μg/ml proteinase K at 56°C and precipitated with isopropanol. In other cases, RNA was extracted from sorted cells from primary tumors or cultures with TRIzol reagent (Invitrogen) according to the manufacturer's guidelines. cDNA was then obtained from 500 ng of RNA using the iScript (Bio-Rad Laboratories, Hercules, CA) retrotranscription kit. Quantitative real-time polymerase chain reaction (PCR) was performed on 10 ng of genomic sample or 1:100 of the retrotranscription reaction using iQ SYBR Green Supermix (Bio-Rad Laboratories). The presence of the proviral insert was determined using a pair of primers specific for GFP amplification, whereas the amplification level of the *Fyn* gene (MGI:95602) was used as reference for data normalization because it has no pseudogenes. mRNA quantifications were normalized to the housekeeping gene *Rpl41* (NM_018860). The sequences of the primers are available on request.

Results

Transduction of PDGF-B in Embryonic Precursors Provokes Tumors Resembling Oligodendrogliomas

We injected replication-deficient retroviruses carrying both PDGF-B– and GFP-coding sequences into the lateral ventricles of the telencephalon in mouse embryos at mid neurogenesis (embryonic day 14; E14). After birth, the injected mice were monitored and killed as soon as they showed symptoms of neurologic distress, which appeared in all injected animals within 190 days (n = 46; Figure 1*A*). In contrast, no mice ever developed gliomas when injected with a control virus (n = 15). The analysis of the brains explanted from PDGF-B–injected animals showed, invariably, masses of GFP-positive cells, indicating a large proliferation of cells that had integrated the PDGF-B–expressing retrovirus (Figure 1*B*).

A more accurate analysis of the survival curve showed that mice developed symptoms with different latency, roughly classifiable in two groups: early-affected and late-affected mice (Figure 1*A*). Early-affected mice often displayed hydrocephaly and weight loss within 2 to 8 weeks after birth with an average of 37 ± 2 days. In most cases, the severe hydrocephalic condition was the likely cause of the symptoms. On histologic analysis, these brains showed broad infiltration of GFP-positive cells within an average volume of 7 ± 4 mm^3, without displaying the typical signs of high-grade gliomas, such as widespread necrosis or massive neovascularization (Figure 1, *C*, *E*, and *E′*), and for this reason, we herein refer to these cellular hyperplasias as low-grade tumors.

In contrast, the late-affected animals exhibited symptoms, ranging from hyperreactivity to imbalanced stance and gait, within 70 to 190 days after birth with an average of 136 ± 13 days, and developed large GFP-positive tumor masses, with an average volume of 65 ± 10 mm^3, without showing hydrocephalous. Most of these brains (15/16) showed wide hemorrhagic regions, were extensively infiltrated, and harbored wide and highly cellularized areas, with clear necrotic regions surrounded by pseudopalisades and newly formed blood vessels (Figures 1, *D*, *F*, and *F′* and W1), all typical signs of high-grade gliomas [1]. In some cases, the tumor mass had completely invaded and almost replaced normal tissues in areas such as the ventral telencephalon and the thalamus (Figure 1*D*).

Owing to the striking difference in the volume of the infiltrated regions (about an order of magnitude), low- and high-grade tumors can be readily distinguished by a macroscopic inspection of the brain on a blue light transilluminator allowing visualization of the GFP. The presence of hemorrhagic regions within the GFP-positive areas could be used as an additional macroscopic criterion to identify high-grade tumors.

Immunohistochemical analysis showed that transduced cells in low- and high-grade tumors did not express either astroglial or neuronal markers, being devoid of GFAP and NeuN (Figure 2, *A*, *B*, *I*, and *J*). Transduced cells expressed the proliferative marker Ki67 (Figure 2, *C* and *K*) and progenitor/stem cells markers such as the intermediate filament Nestin [20], suggesting that they were not fully differentiated (Figure 2, *D* and *L*). They also widely expressed oligodendrocyte lineage–specific markers such as the bHLH transcription factor Olig2 [21] (Figure 2, *E* and *M*), the proteoglycan NG2 [22] (Figure 2, *F* and *N*), the PDGFRα (Figure 2, *G* and *O*), and the form of the APC gene product recognized by the CC1 antibody [23] (Figure 2, *H* and *P*).

This analysis shows that the tumors generated by embryonic transduction of PDGF-B are composed of cells showing unambiguous traits of the oligodendroglial lineage, suggesting that they all represent different grades of oligodendrogliomas and corroborating the notion that some glioblastomas with oligodendroglial component could indeed represent "grade IV oligodendroglioma" [3].

Only High-grade Tumors Induced by PDGF-B Are Tumorigenic When Transplanted

Platelet-derived growth factor B–transduced cells in both high- and low-grade tumors showed high proliferation activity (Figure 2, *C* and *K*), as demonstrated by the percentage of Ki67-positive cells, approximately 20%, among the transduced population [24]. However, we noticed that high-grade tumors, identified through macroscopic inspection as described previously, gave rise in extremely short times to secondary gliomas in 73% of intracranially transplanted adult animals (38 ± 9 days; n = 15 from six independent primary tumors), whereas low-grade tumors, despite a similar expression profile and proliferative activity, failed to cause any sign of illness following

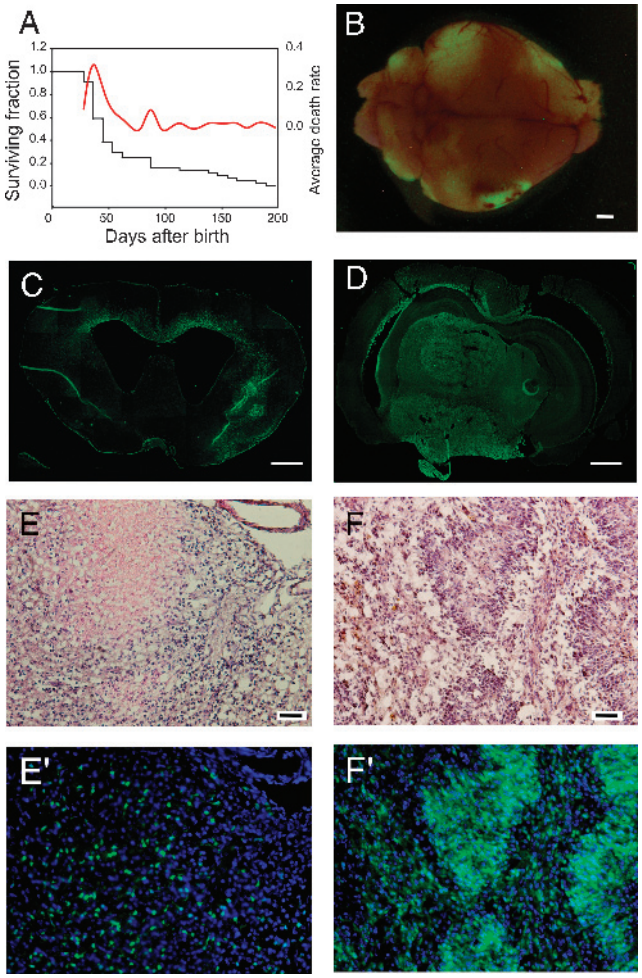

Figure 1. PDGF-B–induced brain tumors with high efficiency. (A) Survival curve (black line) and average death rate plot (dead animal per day, red line) for primary tumors induced by PDGF-B overexpression. (B) Merged fluorescence and brightfield images of a typical high-grade primary tumor. (C–F′) Coronal sections of primary low-grade (C, E, and E′) and high-grade (D, F, and F′) tumors stained with anti-GFP antibody in green (C, E′, D, and F′) or hematoxylin and eosin (E and F). Corresponding fluorescence and bright field microphotographs (E–E′ and F–F′) were taken from the same sections after each staining step. Scale bars, 1 mm (B–D); 100 μm (E–F′).

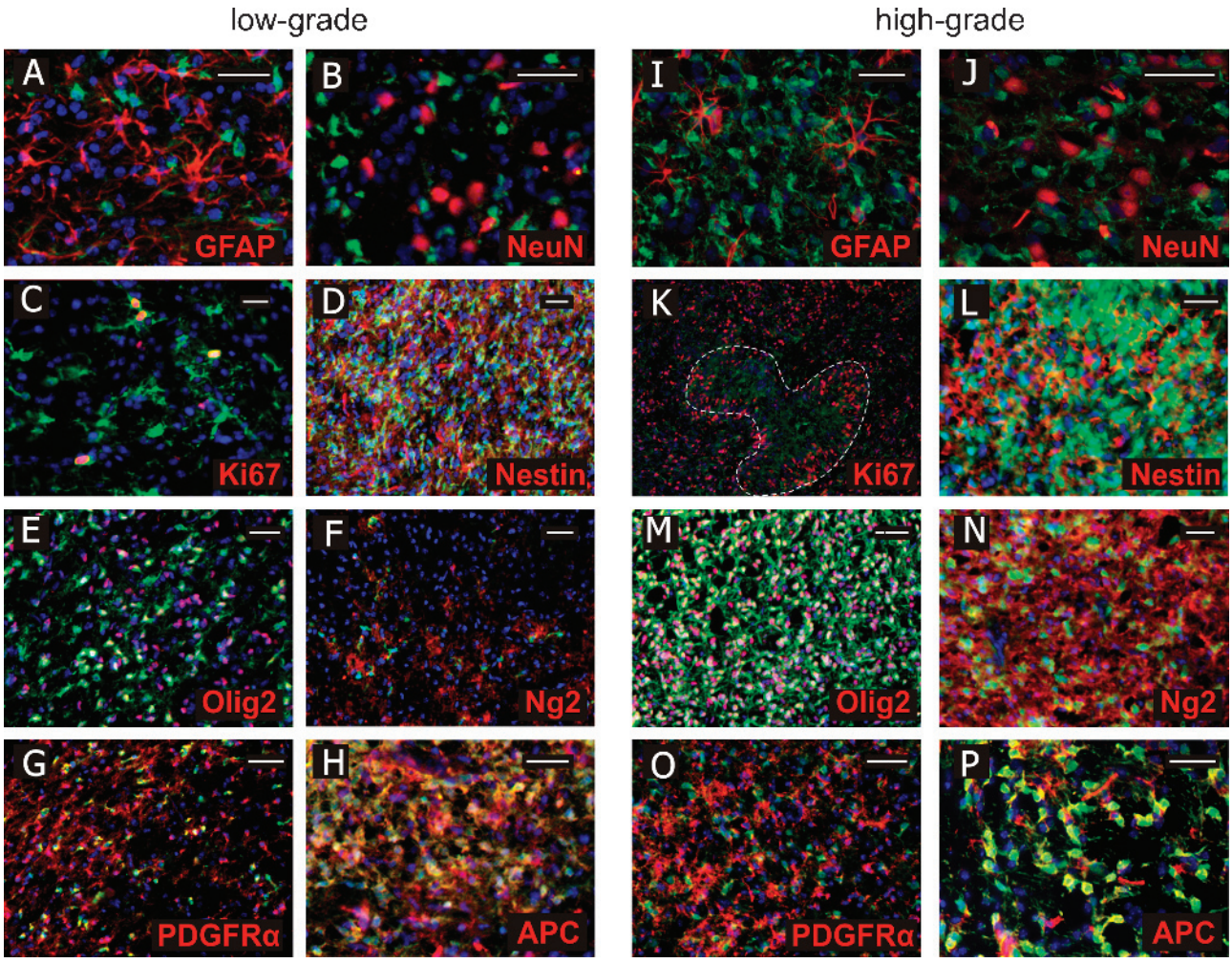

Figure 2. PDGF-B overexpression induced tumor resembling oligodendrogliomas. (A–P) Immunofluorescence stainings of low- (A–H) and high-grade (I–P) tumor sections with anti-GFP antibody in green, DAPI for nuclear staining in blue, and the antibody for the indicated antigen in red. (K, dashed contour) A pseudopalisading structure in a high-grade tumor is shown. Scale bars, 50 μm.

the same experimental paradigm (n = 13 from five independent primary tumors; Figure 3*A*). The secondary tumors generated by intracranial transplantation of high-grade glioma cells resembled their parental counterparts, but they displayed a more compact structure, surrounded by reactive astrocytes (Figure 3*B*), whereas primary tumors typically harbored also a cellular fraction extensively infiltrating the surrounding brain regions. Like their high-grade primary sources, secondary tumors were extremely vascularized and showed wide necrotic areas surrounded by highly proliferating cells forming pseudopalisades (data not shown).

To further evaluate the ability of the tumorigenic component to self-renew during long periods, we serially transplanted secondary tumors into the brain of adult mice. This resulted in the generation of tertiary tumors that showed no obvious difference to their secondary sources in the symptoms onset and proliferative index (data not shown).

High-grade Tumors Can Be Grown in Culture During Long Periods Maintaining Their Tumorigenic Potential and Molecular Phenotype

The difference between low- and high-grade tumors was also reflected by their different abilities to be propagated in culture. Approximately 80% (n = 12) of high-grade tumors, identified by macroscopic inspection, were successfully maintained *in vitro* after dissociation, whereas dissociated cells from low-grade tumors (n = 12) invariably tended to differentiate and eventually die within a few days after plating. High-grade tumors were cultured efficiently for more than 20 passages, without any obvious change in their morphology and proliferative potential. Similarly to their *in vivo* tumor counterparts, cultured cells from high-grade tumors almost never expressed the astrocytic marker GFAP, whereas they were immunopositive for oligodendroglial markers such as Olig2, APC, and NG2 and for the immature neural progenitor marker Nestin (Table W1 and Figure 3*C*).

When cultured cells from independent high-grade tumors were tested for their tumorigenic potential by intracranial reinjections, they all gave rise to secondary tumors, with an average efficiency of 87 ± 9% (five independent tumors, $n \geq 3$ injected mice per tumor; Figure 3*A*). Secondary tumors displayed similar histopathology and latency (on average, 39 ± 3 days) compared to those generated when reinjecting acutely dissociated cells from high-grade tumors.

A gross estimation of the proportion of tumor-initiating cells within the culture of one representative tumor was obtained by applying the Spearman-Kärber formula [25] to the results of a serial logarithmic dilution/transplantation assay, and it revealed that transplantation of

as few as 140 cells would cause a tumor in half of the animals (i.e., DL_{50} = 140; n = 12 animals, four dilutions).

These data indicate that high- and low-grade PDGF-B–induced oligodendrogliomas, despite the similarities at the immunohistochemical and proliferative levels, differ markedly in that only high-grade tumors are able to self-renew extensively *in vivo* and *in vitro*, giving rise to new high-grade gliomas in short times. Altogether, these observations demonstrate that PDGF-B overexpression is alone

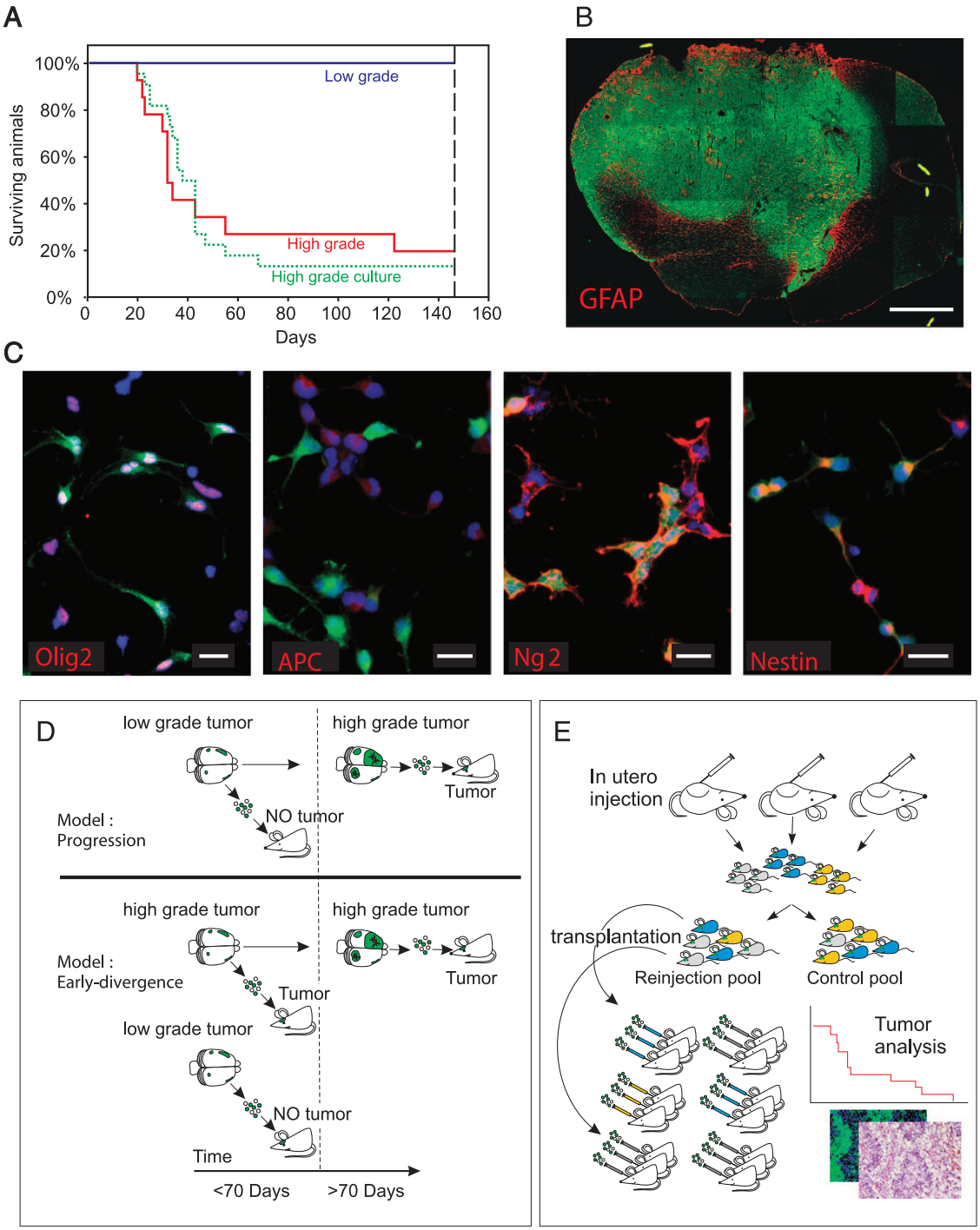

Figure 3. High-grade tumors are tumorigenic and can be propagated in culture. (A) Survival curves for animals transplanted with cells from low-grade (blue line) or high-grade (red line) acutely dissociated primary tumors and cultured high-grade tumor cells (green dotted line). (B) Fluorescence microphotograph of a coronal section of a secondary tumor (green) showing encapsulation by GFAP-expressing astrocytes (anti-GFAP antibody in red). (C) Immunofluorescence stainings of cultured cells from PDGF-B–induced tumors with anti-GFP (green) antibody, DAPI for nuclear staining (blue), and antibodies for the indicated neural lineage markers (red). Scale bars, 1 mm (B); 25 μm (C). (D) Alternative scenarios for the acquisition of malignancy during PDGF-B–induced gliomagenesis. Tumorigenic potential may be either acquired by progression (upper panel) or possessed from the onset (lower panel). (E) Design of the experiments for testing the proposed hypotheses by challenging the ability to generate secondary tumors of cells derived from randomly sorted pups injected with PDGF-B retrovirus.

insufficient to provide glial progenitors with a full-blown tumorigenic potential, as shown by the lack of such character in low-grade PDGF-B–expressing tumors, hence suggesting that PDGF-B–induced tumors may follow a progression path culminating in the generation of extremely aggressive forms. Alternatively, the two forms of tumor might reflect an early difference, produced at the time of the infection.

PDGF-B–Induced Gliomas Progress from Low to High Grade

To distinguish between the two alternatives, we asked if the tumors fated to show high-grade characteristics possess the capability of generating secondary tumors already at early times (i.e., when the low-grade ones become symptomatic) or if they acquire this ability only later by progression (Figure 3*D*). Ideally, addressing this question would require the analysis of the tumorigenic potential of cells derived from a series of early stage tumors and the ability to follow the development of the very same tumors in the animals from which they have been explanted. This strategy would imply the ability to resect part of an early tumor, broadly infiltrated in the brain parenchyma, allowing the animal to survive for one or two additional months. Although this approach would formally allow assessing whether tumors that later will show malignant features are already tumorigenic at early stages, it is not feasible in the mouse. However, we reasoned that it could be adapted by taking advantage of inferential statistics.

From our experiments, we knew that high-grade tumors arise in approximately 40% of mice injected with PDGF-B at embryonic stages. We therefore randomly sorted the pups of eight independent litters injected with PDGF-B viruses defining two similarly sized pools (n = 13 and n = 14 mice), which were used as a source of cells ("reinjection pool") and as a reference ("control pool"), respectively (Figure 3*E*).

The control pool was left untouched, and the animals were killed at the onset of the first symptoms, annotating the latency and the histopathology of the tumors. All the members of the reinjection pool were killed approximately 30 days after birth (29 ± 3 days), around the mortality peak of low-grade tumors, and the GFP-positive regions found in their brains were dissected. At the time of the sacrifice, only 5 of 13 (approximately 40%) mice already displayed symptoms, but tumor masses were present in all the brains. These masses appeared similar in size and distribution, and all yielded several thousand GFP-positive cells when dissociated. Six independent injections (n = 78) were then performed for every tumor (n = 13), using $1 \pm 0.3 \times 10^4$ GFP-positive cells per injection. Notably, the number of transplanted cells in this experiment was about two orders of magnitude higher than the median lethal dose derived from experiments using the cultured cells (i.e., 140 cells; see previous paragraphs). Thus, if some GFP-positive mass harbored already tumorigenic cells, we would expect them to give rise to secondary tumors in a very short time, similar to the reinjection of late-onset high-grade tumors.

None of the animals receiving GFP-positive cells developed any tumor, regardless of whether the donors were symptomatic or not. This was in striking contrast with the ability of late-onset high-grade PDGF-B–induced gliomas to give rise to secondary tumors with high efficiency even after injection of only a few hundred cells. In contrast, approximately 50% of the control pool displayed high-grade histopathology and late onset. Assuming the percentage of tumors destined to become high-grade gliomas to be approximately the same in the two pools, we expected approximately seven mice within the reinjection pool to be fated to develop a high-grade tumor. This observation demonstrates that, at early stages, the tumors induced by PDGF-B overexpression are equivalent, lacking the potential to generate secondary tumors. The malignancy shown by late-onset tumors is therefore a peculiar property acquired by progression.

A preliminary analysis aimed at identifying possible gene expression alterations responsible for the progression was carried out by comparing the expression levels of a limited number of candidate genes in low- and high-grade tumors by real-time PCR. This analysis leads to the identification of the gene *Btg2*, whose expression is significantly lower in high-grade PDGF-B–induced gliomas compared to low-grade ones (Figure 4*A*). These data show a strong correlation between the acquisition of tumorigenic potential by PDGF-B–induced gliomas and the down-regulation of *Btg2*, which may play a role as a tumor suppressor in this context. In agreement with this possibility, *Btg2* acts as an oncosuppressor in medulloblastoma, another central nervous system tumor [26], and its deregulation has been suggested to cooperate with PDGF-B in driving the formation of gliomas [27,28].

Fully Progressed Tumor Cells Are Addicted to PDGF-B

Inspection of high-grade tumor cultures revealed the presence of a substantial population of GFP-negative cells, which showed a marker expression profile similar to that of GFP-positive cells (Table W1). Notably, GFP-negative cells were able to proliferate extensively in culture also in the absence of the PDGF-B paracrine support from the GFP-positive fraction, after FACS purification, suggesting they underwent the same progression pathway as the GFP-positive cells. Accordingly, the level of *Btg2* mRNA in GFP-negative cultures was similar to the level of their PDGF-B/GFP-positive counterparts and to acutely dissociated high-grade tumors (Figure 4*A*).

The similarity between GFP-positive and -negative cells, together with the observation that GFP-positive clones obtained by multiple dilutions generate a fraction of GFP-negative cells (data not shown), prompted us to clarify if the GFP-negative population represents recruited cells or if it derives from GFP-positive cells by silencing of the proviral promoter. We therefore performed a real-time PCR analysis to evaluate the presence of the integrated provirus into the genome of the sorted GFP-negative cells. Our analysis showed that both GFP-positive and -negative cells contain the same amount of provirus in their genomes (Figure 4*B*), strongly supporting the hypothesis of the provirus transcriptional silencing.

Despite their similarities, cultured GFP-positive and GFP-negative cells dramatically differed in their ability to give rise to new tumors when challenged with *in vivo* reinjections experiments. Cultured GFP-positive cells from all tumors tested were able to give rise to secondary gliomas with an average efficiency of 78 ± 15% (n = 18; Figure 4*C*). On the contrary, the GFP-negative fraction invariably failed to do so even after injecting as many as 50,000 cells (more than two orders of magnitude more than the estimated DL_{50} for GFP-positive cells, see previous paragraphs; n = 12, Figure 4*C*). These results, together with the observation that the GFP-negative fraction derives from GFP-positive cells, strongly suggest that high-grade glioma cells, although progressed to a highly malignant state, had not become independent from PDGF-B signaling for their ability to propagate as tumors *in vivo*. To further confirm that tumorigenic potential depends on PDGF-B overexpression, we reinjected adult mouse brains with cultured GFP-negative cells 2 days after their transduction with a retroviral vector expressing PDGF-B in association with the red fluorescent protein Ds-Red. These cells proved able to induce the formation of secondary gliomas with the same efficiency of the GFP-positive counterpart, demonstrating that the observed differences in tumorigenic potential between GFP-positive

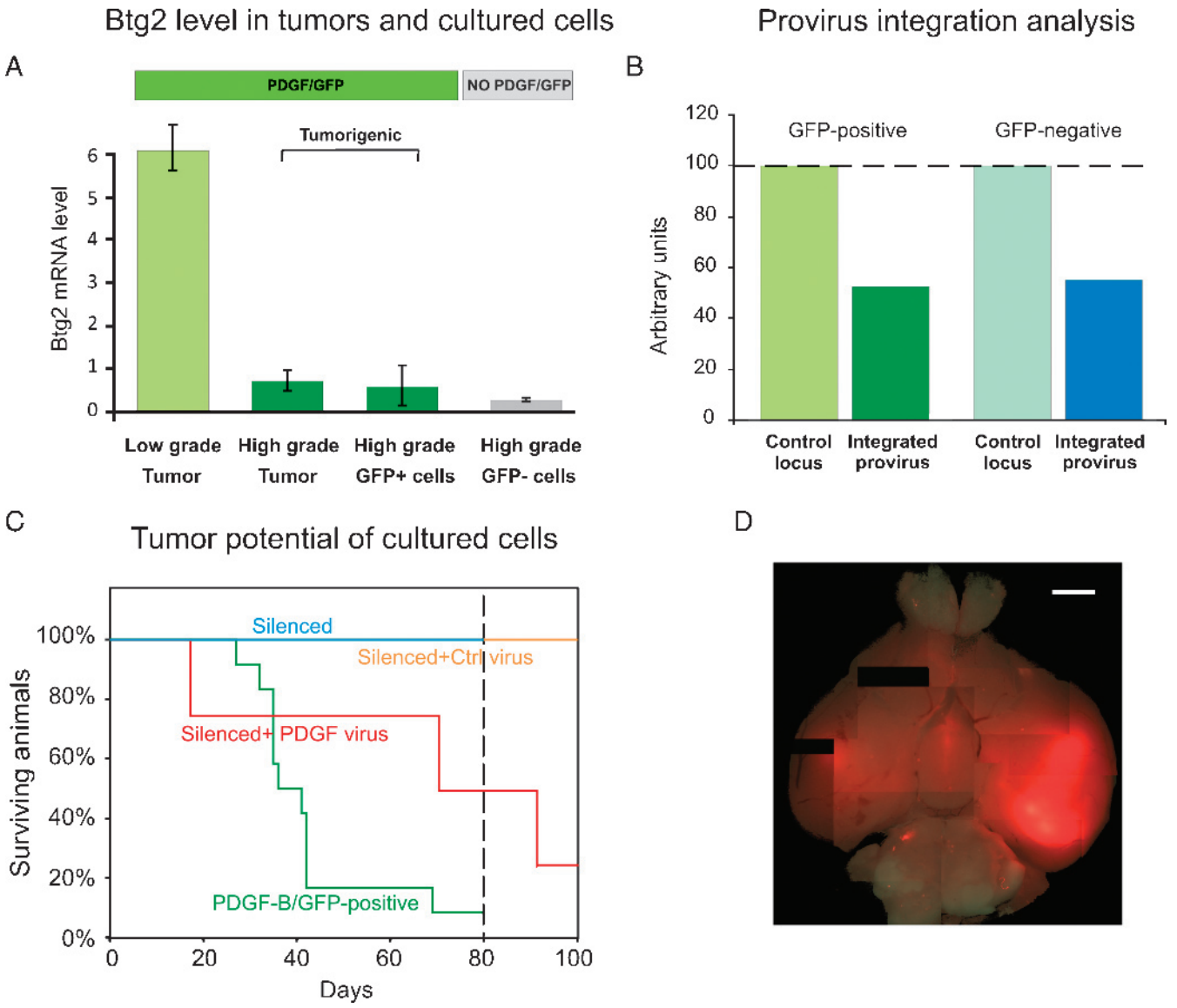

Figure 4. *Btg2* is down-regulated in high-grade tumors that are addicted to PDGF-B. (A) Histogram shows the levels of *Btg2* mRNA as percentage of the level of the housekeeping gene *Rpl41* in FACS-purified cells from primary tumors or cultured cells as indicated. Values represent the means of real-time PCR quantifications for three independent tumors per condition. (B) Histogram shows the amount of the integrated provirus in the genome of transduced GFP-positive and GFP-negative cells normalized to the amount of the Fyn locus. (C) Survival curves for transplantation experiments using cultures of sorted GFP/PDGF-B–positive cells and of silenced (GFP-negative) cells either untreated or reinfected with a PDGF-B–expressing or control virus. (D) Merged fluorescence and bright-field photographs of a secondary tumor induced by silenced cells upon transduction with a PDGF-B/Ds-Red–expressing vector. Scale bar, 2 mm.

and GFP-negative cells could be entirely accounted for by the silencing of PDGF-B expression (Figure 4, *C* and *D*). The prompt loss of tumorigenic potential on transgene inactivation demonstrates that high-grade PDGF-B–induced gliomas are addicted to their triggering oncogenic stimulus, despite the progression they have undergone.

Cellular Mechanisms Underlying PDGF-B Addiction

Having established that PDGF-B–induced high-grade gliomas strictly depend on PDGF-B overexpression for maintaining their potential to form tumors *in vivo*, we went on to investigate the cellular mechanisms underlying this phenomenon.

As previously mentioned, cells that have lost PDGF-B overexpression by proviral silencing can be cultured and expanded without the paracrine support of the PDGF-B–overexpressing cells and in the absence of added growth factors (data not shown). This indicates that PDGF-B overexpression is dispensable for the *in vitro* proliferation of cells deriving from these gliomas, revealing that cells that have progressed to malignancy are independent from the triggering oncogenic stimulus for their ability to proliferate in culture. This also indicates that the dependency on PDGF-B overexpression for the *in vivo* tumorigenic potential (oncogene addiction) may not reside in a requirement for PDGF-B as a mitogenic stimulus. To evaluate if and to which extent the expression of PDGF-B may influence the proliferative potential of glioma cells, we performed growth curve analyses on cultures of GFP-positive and GFP-negative cells established from two independent primary high-grade tumors. The analyses confirmed the ability of both

cell populations to proliferate extensively before reaching confluence, as also shown by their similar percentage of cells incorporating BrdU during a 24-hour pulse: 75 ± 5% (number of cells = 1967) for the GFP-positive and 78 ± 5% (number of cells = 2794) for the GFP-negative cells. However, a striking difference between these cell populations became evident after reaching confluence, wherein PDGF-B–expressing cells grew exponentially for at least 24 additional hours, whereas the silenced population showed a sharp decrease in its growth rate (Figure 5*A*). Most remarkably, PDGF-B–overexpressing cells eventually formed massive foci, whereas GFP-negative (PDGF-B–silenced) cells invariably failed to do so (Figure 5, *B* and *C*). Importantly, the reintroduction of PDGF-B by using a Ds-Red–encoding retrovirus in the GFP-negative cells reestablished their ability to undergo unconstrained cell proliferation, eventually resulting in the formation of foci (Figure 5, *A*, *D*, and *E*).

Altogether, these data demonstrate that PDGF-B overexpression allows cells to overcome the cell-cell contact–mediated inhibition of proliferation and eventually display the ability to form foci, a property often correlating with the tumorigenic potential of transformed cells.

Along with the ability to overcome contact inhibition of proliferation, malignant cells typically show the propensity to infiltrate surrounding tissues. This is particularly true for gliomas that are almost untreatable also owing to their marked tendency to infiltrate the brain parenchyma. We therefore tested if PDGF-B overexpression may correlate with the ability of cells to infiltrate the brain. Platelet-derived growth factor B–overexpressing cells (number of cells = 1500) were cotransplanted into adult mouse brains (n = 7) together with PDGF-B–silenced cells labeled with a control retroviral vector coding for Ds-Red (number of cells = 3500). We then killed two animals at both 1 and 2 weeks after transplantation and allowed the others to develop tumors before killing them. Sections from 1- and 2-week-old brains revealed needle tracks containing weakly autofluorescent densely packed cells. At 1 week after injection, both GFP-positive and Ds-Red–positive cells were clearly visible around the needle track of all the brains examined (n = 2; Figure 5*F*); however, unsurprisingly, their number was much lower than that of injected cells. A striking observation was that, whereas the distribution of Ds-Red-expressing cells was limited to the needle track, the PDGF-B–overexpressing cells were found mostly outside the track and as far as in the contralateral hemisphere (data not shown). Two weeks after injection, the only detectable transplanted cells were Ds-Red–positive and they were confined to the needle track. Importantly, no GFP-positive cells were visible either inside or near the injection site, suggesting that the few surviving cells had scattered in a larger volume. All the remaining animals were killed after another 30 to 50 days because of the development of gliomas that were found to be exclusively GFP-positive. These observations show that only a minority

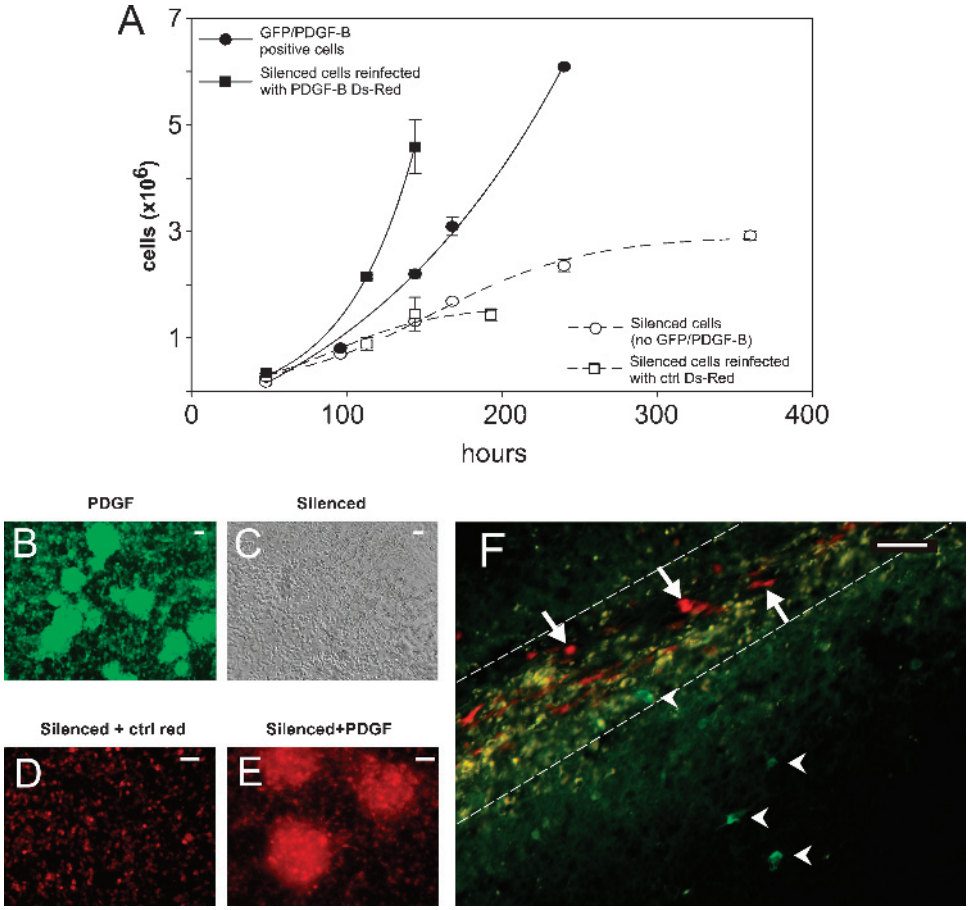

Figure 5. (A) Representative growth curves of cultured high-grade tumor cells either expressing PDGF-B or not. (B–E) Fluorescence microphotographs of cultured cells at confluence showing the focus formation: PDGF-B/GFP–expressing cells (B), PDGF-B–silenced cells (C), PDGF-B–silenced cells reinfected with a Ds-Red control virus (D), PDGF-B–silenced cells reinfected with a PDGF-B/Ds-Red virus (E). (F) Coronal section at the injection site 1 week after transplantation showing PDGF-B/GFP–positive cells (green, arrowheads) and PDGF-B–silenced cells infected with a Ds-Red control virus (red, arrows); dashed lines indicate the limit of the needle track. Scale bar, 50 μm.

of tumor cells survive the graft and, most importantly, that PDGF-B overexpression and tumorigenic potential correlate with the *in vivo* ability of glioma cells to scatter through the surrounding brain parenchyma. Indeed, silenced cells lack both the ability to infiltrate the surrounding tissues and to form tumors upon transplantation. The rapid decrease in the number of injected cells and the fast dispersal of the GFP-positive cells through the brain that we observed in the first 2 weeks after injection are likely the reasons why the PDGF-B expressed from the GFP-positive cells failed to paracrinally support the growth and/or the survival of the Ds-Red-expressing cells. This therefore explains why the tumors resulting from the cotransplantations did not contain a Ds-Red–positive component.

Discussion

In our attempt to characterize a model of gliomagenesis, we have found that PDGF-B overexpression in telencephalic mouse neural progenitor cells is highly efficient at inducing tumors. These tumors comprise low- and high-grade forms, all sharing markers of the oligodendroglial lineage, even when displaying histopathologic traits typical of glioblastoma, such as extended necrosis, pseudopalisades, and widespread angiogenesis. This observation indirectly supports the notion that some of the tumors named "glioblastomas with oligodendroglioma component" in the last revision of the World Health Organization classificatory scheme [3] could indeed be considered as "grade IV oligodendroglioma."

Tumors induced by embryonic transduction of PDGF-B comprised a subgroup that was lethal within a few weeks after birth. Despite this very aggressive behavior, early neoplasias possessed histopathologic and functional properties that unambiguously allowed their classification as low-grade tumors. Most prominently, these gliomas, which could not be maintained in culture, were devoid of any sizable tumor-initiating subpopulation, as demonstrated by our *in vivo* transplantation experiments. Early tumors were completely unable to propagate themselves when reinjected intracranially, even when a high number of cells were transplanted.

A relevant proportion of the PDGF-B–induced gliomas, characterized by longer latency, emerged as histopathologically and functionally highly malignant forms, ultimately causing the death of all injected animals within a few months after birth. These forms could be efficiently propagated *in vivo* in serial transplantation assays and showed the potential for long-term *in vitro* culturing with no alteration in their tumorigenic potential, as demonstrated by highly successful intracranial reinjections using cultured tumor cells.

We used an inferential statistics approach to demonstrate that high-grade tumors derive from nontumorigenic cells that, only later, acquire tumorigenic potential. This shows that PDGF-B is able to drive the formation of low-grade tumors that need to acquire further lesions to progress toward malignancy. This experimental paradigm represents, therefore, an *in vivo* model of glioma progression.

As a possible candidate responsible for the observed progression, we identified *Btg2*, which is strongly down-regulated in high-grade tumors compared to low-grade ones. *Btg2* is an interesting candidate because it has been suggested to cooperate with PDGF-B overexpression in driving the formation of gliomas [27] and because it acts as an oncosuppressor in medulloblastoma [26].

Our data show that, at least in this context, neither the overexpression of PDGF-B nor the down-regulation of *Btg2* are alone sufficient for a cell to be tumorigenic. This is demonstrated by the lack of malignancy of both PDGF-B–overexpressing low-grade tumors and PDGF-B–silenced high-grade tumor cells (that show a low level of *Btg2*). Rather, tumorigenicity is a characteristic exhibited by cells displaying, at the same time, PDGF-B overexpression and low *Btg2* level. Altogether, these observations suggest that *Btg2* may represent a relevant tumor suppressor in the context of PDGF-B–induced gliomagenesis and that its down-regulation is an important step during tumor progression.

Our observation that cells silencing the proviral expression of PDGF-B impairs tumorigenic potential shows that PDGF-B overexpression, albeit alone insufficient to confer malignancy, is necessary for the maintenance of this feature in high-grade tumors. Such oncogene addiction [29] was further confirmed by the reintroduction, into silenced cells, of a new PDGF-B–expressing vector, which rescued their tumor-propagating ability. Although other authors already showed that the development of PDGF-B induced tumors is dependent on continuous PDGF-B signaling [30,31], our data represent the first demonstration that fully progressed tumors remain addicted to their triggering oncogenic stimulus. If this is lost, cells completely lose the ability to generate secondary tumors. As soon as it is restored, cells reacquire full tumorigenic potential.

Cells undergoing proviral silencing, while losing the ability to propagate as tumors *in vivo*, maintained a very similar molecular phenotype and a very high proliferative potential *in vitro*. These observations show, on the one hand, that during progression from low- to high-grade tumors, cells must have accumulated additional alterations allowing them to proliferate abnormally and, on the other, that the *in vitro* proliferative activity does not necessarily correlate with the ability to regenerate a glioma on transplantation *in vivo*. Remarkably, we found that the ability to overcome cell-cell contact–mediated growth-inhibitory stimuli correlated with the tumorigenic potential of these cells. We indeed demonstrate that PDGF-B overexpression plays a crucial role in this process. Platelet-derived growth factor B–overexpressing cells were not sensitive to growth-inhibitory stimuli induced by cell-cell contacts and eventually formed foci, whereas silenced cells lacked the ability to grow past confluence and reacquired it as soon as PDGF-B overexpression was reestablished.

Altogether, our data demonstrate that PDGF-B overexpression supports the formation and progression of oligodendrogliomas toward highly malignant forms. We also show that cells from fully progressed tumors remain dependent on PDGF-B overexpression for their tumorigenic potential. Our data suggest that the addiction to PDGF-B might be connected to its requirement for suppressing cell-cell contact growth-inhibitory signals. Moreover, our observations suggest a role for PDGF-B in the invasive capability of glioma cells, showing that the PDGF-B overexpression confers cells the ability to infiltrate the surrounding tissues.

Our data support the concept that, even in patients bearing highly malignant tumors that have accumulated multiple molecular lesions, therapies targeting a prominent oncogene may prove effective for limiting tumor growth and relapse.

References

[1] Furnari FB, Fenton T, Bachoo RM, Mukasa A, Stommel JM, Stegh A, Hahn WC, Ligon KL, Louis DN, Brennan C, et al. (2007). Malignant astrocytic glioma: genetics, biology, and paths to treatment. *Genes Dev* **21**, 2683–2710.

[2] Louis DN, Holland EC, and Cairncross JG (2001). Glioma classification: a molecular reappraisal. *Am J Pathol* **159**, 779–786.

[3] Louis DN, Ohgaki H, Wiestler OD, Cavenee WK, Burger PC, Jouvet A, Scheithauer BW, and Kleihues P (2007). The 2007 WHO classification of tumours of the central nervous system. *Acta Neuropathol* **114**, 97–109.

[4] Lyustikman Y, Momota H, Pao W, and Holland EC (2008). Constitutive activation of Raf-1 induces glioma formation in mice. *Neoplasia* **10**, 501–510.
[5] Shih AH and Holland EC (2006). Platelet-derived growth factor (PDGF) and glial tumorigenesis. *Cancer Lett* **232**, 139–147.
[6] Di Rocco F, Carroll RS, Zhang J, and Black PM (1998). Platelet-derived growth factor and its receptor expression in human oligodendrogliomas. *Neurosurgery* **42**, 341–346.
[7] Hermanson M, Funa K, Hartman M, Claesson-Welsh L, Heldin CH, Westermark B, and Nister M (1992). Platelet-derived growth factor and its receptors in human glioma tissue: expression of messenger RNA and protein suggests the presence of autocrine and paracrine loops. *Cancer Res* **52**, 3213–3219.
[8] Nister M, Libermann TA, Betsholtz C, Pettersson M, Claesson-Welsh L, Heldin CH, Schlessinger J, and Westermark B (1988). Expression of messenger RNAs for platelet-derived growth factor and transforming growth factor-alpha and their receptors in human malignant glioma cell lines. *Cancer Res* **48**, 3910–3918.
[9] Dai C, Lyustikman Y, Shih A, Hu X, Fuller GN, Rosenblum M, and Holland EC (2005). The characteristics of astrocytomas and oligodendrogliomas are caused by two distinct and interchangeable signaling formats. *Neoplasia* **7**, 397–406.
[10] Holland EC, Celestino J, Dai C, Schaefer L, Sawaya RE, and Fuller GN (2000). Combined activation of Ras and Akt in neural progenitors induces glioblastoma formation in mice. *Nat Genet* **25**, 55–57.
[11] Tchougounova E, Kastemar M, Brasater D, Holland EC, Westermark B, and Uhrbom L (2007). Loss of Arf causes tumor progression of PDGFB-induced oligodendroglioma. *Oncogene* **26**, 6289–6296.
[12] Uhrbom L, Dai C, Celestino JC, Rosenblum MK, Fuller GN, and Holland EC (2002). Ink4a-Arf loss cooperates with KRas activation in astrocytes and neural progenitors to generate glioblastomas of various morphologies depending on activated Akt. *Cancer Res* **62**, 5551–5558.
[13] Assanah M, Lochhead R, Ogden A, Bruce J, Goldman J, and Canoll P (2006). Glial progenitors in adult white matter are driven to form malignant gliomas by platelet-derived growth factor–expressing retroviruses. *J Neurosci* **26**, 6781–6790.
[14] Jackson EL, Garcia-Verdugo JM, Gil-Perotin S, Roy M, Quinones-Hinojosa A, VandenBerg S, and Alvarez-Buylla A (2006). PDGFR alpha–positive B cells are neural stem cells in the adult SVZ that form glioma-like growths in response to increased PDGF signaling. *Neuron* **51**, 187–199.
[15] Uhrbom L, Hesselager G, Nister M, and Westermark B (1998). Induction of brain tumors in mice using a recombinant platelet-derived growth factor B-chain retrovirus. *Cancer Res* **58**, 5275–5279.
[16] Pear WS, Nolan GP, Scott ML, and Baltimore D (1993). Production of high-titer helper-free retroviruses by transient transfection. *Proc Natl Acad Sci USA* **90**, 8392–8396.
[17] Heins N, Cremisi F, Malatesta P, Gangemi RM, Corte G, Price J, Goudreau G, Gruss P, and Gotz M (2001). Emx2 promotes symmetric cell divisions and a multipotential fate in precursors from the cerebral cortex. *Mol Cell Neurosci* **18**, 485–502.
[18] Appolloni I, Calzolari F, Corte G, Perris R, and Malatesta P (2008). Six3 controls the neural progenitor status in the murine CNS. *Cereb Cortex* **18**, 553–562.
[19] Malatesta P, Sgado P, Caneparo L, Barsacchi G, and Cremisi F (2001). *In vivo* PC3 overexpression by retroviral vector affects cell differentiation of rat cortical precursors. *Brain Res Dev Brain Res* **128**, 181–185.
[20] Frederiksen K and McKay RD (1988). Proliferation and differentiation of rat neuroepithelial precursor cells *in vivo*. *J Neurosci* **8**, 1144–1151.
[21] Zhou Q, Wang S, and Anderson DJ (2000). Identification of a novel family of oligodendrocyte lineage-specific basic helix-loop-helix transcription factors. *Neuron* **25**, 331–343.
[22] Diers-Fenger M, Kirchhoff F, Kettenmann H, Levine JM, and Trotter J (2001). AN2/NG2 protein–expressing glial progenitor cells in the murine CNS: isolation, differentiation, and association with radial glia. *Glia* **34**, 213–228.
[23] Lu QR, Sun T, Zhu Z, Ma N, Garcia M, Stiles CD, and Rowitch DH (2002). Common developmental requirement for Olig function indicates a motor neuron/oligodendrocyte connection. *Cell* **109**, 75–86.
[24] Gerdes J, Scholzen T, Gerlach C, Kubbutat M, and Zentgraf H (1997). Assessment of cell proliferation in murine tissues with a polyclonal antiserum against the murine Ki-67 protein. *Eur J Cell Biol* **72**, 263.
[25] Hamilton MA, Russo RC, and Thurston RV (1977). Trimmed Spearman-Karber method for estimating median lethal concentrations in toxicity bioassays. *Environ Sci Technol* **11**, 714–719.
[26] Farioli-Vecchioli S, Tanori M, Micheli L, Mancuso M, Leonardi L, Saran A, Ciotti MT, Ferretti E, Gulino A, Pazzaglia S, et al. (2007). Inhibition of medulloblastoma tumorigenesis by the antiproliferative and pro-differentiative gene *PC3*. *FASEB J* **21**, 2215–2225.
[27] Johansson FK, Brodd J, Eklof C, Ferletta M, Hesselager G, Tiger CF, Uhrbom L, and Westermark B (2004). Identification of candidate cancer-causing genes in mouse brain tumors by retroviral tagging. *Proc Natl Acad Sci USA* **101**, 11334–11337.
[28] Johansson Swartling F (2008). Identifying candidate genes involved in brain tumor formation. *Ups J Med Sci* **113**, 1–38.
[29] Sharma SV and Settleman J (2007). Oncogene addiction: setting the stage for molecularly targeted cancer therapy. *Genes Dev* **21**, 3214–3231.
[30] Shih AH, Dai C, Hu X, Rosenblum MK, Koutcher JA, and Holland EC (2004). Dose-dependent effects of platelet-derived growth factor-B on glial tumorigenesis. *Cancer Res* **64**, 4783–4789.
[31] Uhrbom L, Nerio E, and Holland EC (2004). Dissecting tumor maintenance requirements using bioluminescence imaging of cell proliferation in a mouse glioma model. *Nat Med* **10**, 1257–1260.

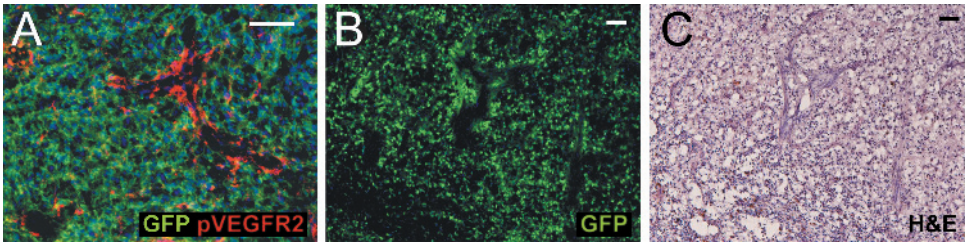

Figure W1. High-grade tumors harbor an aberrant blood vessel network. (A, B) Immunofluorescence staining with antibodies against GFP in green (A, B) and phosphoVEGFR2 in red (A). (C) Hematoxylin and eosin staining of the same section as in (B). Scale bars, 50 μm.

Table W1. Neural Marker Expression in Cultured Tumor Cells.

Marker	Cultured Tumor Cells	
	(a) GFP-Positive	(b) GFP-Negative
GFAP	≪1% (850)	≪1% (900)
Olig2	94 ± 3% (687)	58 ± 14% (774)
APC(cc1)	66 ± 17% (948)	68 ± 18% (1702)
Ng2	92 ± 5% (808)	69 ± 6% (1080)
Nestin	95 ± 2% (849)	70 ± 9% (1472)

The percentage of positivity to the indicated molecular markers ± SE is indicated for both GFP-positive and GFP-negative cultured tumor cells. Data were collected by three independent experiments. In parentheses are indicated the total number of cells counted.